Features of kinetic processes in a dusty plasma induced by a shock wave propagating in the atmosphere

A.M. Starik, A.M. Savel'ev, N.S. Titova and O.E. Rein[1]

[1] *Central Institute of Aviation Motors, Scientific Research Center "Raduga", Aviamotornaya Str. 2, Moscow, 111116 Russia*

Introduction

Upper and middle atmosphere contains different kinds of ions, clusters, and nanoparticles. Shock waves forming in the air over the vehicles crossing the upper and middle layers of the atmosphere with a hypersonic velocity or produced by atmospheric electrical discharges and explosions induce the fast nonequilibrium processes in high temperature plasma behind the shock front. In the most cases the processes in such high temperature plasma are far from being equilibrium.

For past decades a great progress has been achieved in the understanding of different nonequilibrium processes which take place in a high temperature gas behind the leader shock over a spacecraft or aircraft moving in the atmosphere [1, 2]. However, besides molecules, atoms, electrons, and ions the plasma in the post-shock flow may involve different clusters and nanoparticles that present in the background atmosphere (Aitken nuclear, meteoric dust, ionic clusters, and etc.). They also may be formed over the vehicle surface due to ablation or erosion of vehicle thermal protection as well as clustering and aggregation of primary particles. However, up to now in modern studies there is no quantitative information about possible effects of the abundance of clusters and nanoparticles in plasma behind the shock and plasma surrounding the hypersonic vehicle. The purpose of this paper is to analyse the influence of cluster and nanoparticle abundance in a flow behind the shock on the plasma properties.

Methodology

The kinetics of processes behind a shock wave propagating in a gas, in particular, air, is determined by a combination of various phenomena: excitation of the internal (rotational, vibrational, and electronic) degrees of freedom of molecules, dissociation and chemical reactions, ionization and ion-molecular reactions, radiation, variation of the temperature and pressure. The intensity and significance of these processes depend on the initial state of the medium and the velocity of the shock wave or the vehicle velocity, and the way they succeed each other is determined by the hierarchy of the characteristic times and depends on the gas temperature, T, and pressure, p.

At $T \leq 3000$ K and $p > 10^3$ Pa this hierarchy has the form: $\tau_t \leq \tau_r < \tau_V \leq \tau_{ch} \sim \tau_e < \tau_i < \tau_{ph} \sim \tau_R$, where τ_t, τ_r, and τ_V are the characteristic times of translational, rotational, and vibrational relaxation, respectively, τ_{ch}, τ_e, and τ_R are the characteristic times of the chemical reactions, collisional quenching of electronically excited states, the radiative disintegration of excited states, respectively, and τ_i and τ_{ph} are the characteristic times of ionization and photodissociation. With increase in T the difference between τ_V, τ_{ch}, τ_e, and τ_i decreases and at $T \geq 3000$ K behind the shock front the processes of vibrational relaxation, chemical transformation, and quenching (or excitation) of the electronic states of the atoms and molecules, as well as ionization, can occur on the same time intervals (the time τ_R is determined by the probability of spontaneous transition and by the density of the molecules in the excited state and τ_{ph} by the absorption cross-section and the intensity of the radiation absorbed).

At the same time, for shock waves with Mach numbers $M_0 > 2$ for the majority of gases the condition $\tau_t < \tau_r << \tau_V$ is satisfied. This makes it possible to use the gasdynamic approximation in which a shock front is treated as a discontinuity of the gasdynamic parameters and behind the front the change in these parameters is caused by vibrational relaxation processes and chemical reactions.

Consider air shock waves of the intensities such that behind the shock front $\tau_V \leq \tau_{ch} << \tau_e, \tau_R, \tau_i$ and when $\tau_V \leq \tau_{ch} \sim \tau_e \sim \tau_R \sim \tau_i < \tau_{ph}$. The developed kinetic model involves the following neutral excited and

nonexcited species: $O(^3P)$, $O(^1D)$, $O(^1S)$, $O_2(X^3\Sigma_g^-)$, $O_2(a^1\Delta_g)$, $O_2(b^1\Sigma_g^+)$, $O_2(A^3\Sigma_u^+)$, $O_2(B^3\Sigma_u^-)$, O_3, $N(^4S)$, $N(^2D)$, $N(^2P)$, $N_2(X^1\Sigma_g^+)$, $N_2(A^3\Sigma_u^+)$, $N_2(B^3\Pi_g)$, $N_2(a'\Sigma_u^-)$, $N_2(C^3\Pi_u)$, NO, NO_2, N_2O, NO_3 as well as charged species: e, O^+, O^-, O_2^+, O_2^-, O_3^-, O_4^+, O_4^-, N^+, N_2^+, NO^+, NO^-, NO_2^+, NO_2^-, NO_3^-, N_2O^+, N_2O^-, N_3^+, N_4^+. For charged species the list of elementary reactions involves the processes of associative and dissociative ionization, ionization of neutral (including excited atoms and molecules) by electron impact, ionization under molecule and electron interaction, associative electron attachment, nonresonance charge exchange, binary ion-molecular reactions, ion-molecular reactions with electron formation, ternary recombination of ion and neutral, dissociative recombination, ion-electron recombination, binary and ternary ion-ion-recombination. Additionally, we take into account the ion and electron attachment to nanoparticles. In general, the particles that are presented in the atmosphere: Aitken nuclei and meteoric dust have a rather high electrical conductivity. The particles formed during ablation or erosion of the vehicle thermal protection consist of TiO_2 and ZnO monomers and are also conductive.

When the nanoparticles or clusters are abundant in the shock layer or in the gas surrounding the vehicle the additional characteristic kinetic times should be entered into consideration. These ones are the time of particle charging, τ_c, and the time of coagulation of particles or clusters, τ_{co}. For particle with high electrical conductivity we need take into account not only exerting of Coulomb force between ion (electron) and particle but also the image force. The latter comes into existence due to polarization of conducting particle in an electric field created by ion. The interaction potential between the ion (electron) and a metallic particle has the form:

$$\varphi(r) = \frac{Pe^2}{r} - \frac{e^2 a^3}{2r^2(r^2 - a^2)}.$$

(1)

Here, P is the product of the charges of the ion and particle, r is the distance between the ion and soot particle, e is the elementary charge, and a is the radius of the soot particle. The fundamental difference of the interaction described by potential (1) from Coulomb interaction is that the soot particle can capture the ion at distances $r_\Delta > a$. If the ion approaches the soot particle at a distance smaller than r_Δ, its trajectory has the spiral form. The polarization of particle makes it possible to acquire a few electrons (ions) by particle [3].

In the expression (1) the first term is the Coulomb potential and the second term is the image potential. If the particle consists of material with dielectric permeability ε the image potential is not given by a simple analytical formula. In this case the expression for the image potential can be found as

$$\varphi_{image}(r) = -\frac{e^2}{2}(\varepsilon - 1)\sum_{n=1}^{\infty} \frac{na^{2n+1}}{(n(\varepsilon+1)+1)r^{2n+2}} P_n(\cos\theta = 0)$$

where $P_n(\cos\theta)$ are the Legendre polynomials of the nth order.

The attachment coefficient for ion-particle interaction is calculated in the same manner as in ref. [3]. We took into account that particles may have different sizes and that particles with given radius can differ in the accumulated charge, q. The methodology of the description of charging and discharging events in a bipolar ion (electron) environment has been developed previously [3].

We will analyse the flow in which a gas moving with the velocity u_0 (zero subscripts correspond to the undisturbed flow parameters) interacts with an oblique shock wave located at an angle $\beta \leq 90°$ to the vector u_0. Let us assume that $\tau_r \approx \tau_t$ and there is a thermodynamic equilibrium between the rotational and translational degrees of freedom. Consider, at first, the case when there are no any particles in the ambient atmosphere and in the shock layer. Behind the shock front the equilibrium between translational and vibrational degrees of freedom is violated and at $\tau_V \leq \tau_{ch}$ chemical reactions take place under nonequilibrium conditions. At not very high temperatures for the lower vibrational levels of each mode the Boltzmann molecular distribution is practically inviolated. This makes it possible to use the local vibrational temperature model [4, 5] to describe the relaxation processes.

Within the framework of the assumptions accepted above the chemical reaction rate constant is a function of T_j and T:

$$k_q(T, T_j) = \varphi_q(T, T_j) k_q^0(T).$$

Here, $k_q^0(T)$ is the qth chemical reaction rate constant at $T_j=T$, T_j is the vibrational temperature of jth mode, and $\varphi_q(T, T_j)$ is the nonequilibrium factor. It is worth to note that there are several models for estimation of $\varphi_q(T, T_j)$ factor obtained within the framework of the two-temperature approximation in which only one vibrational temperature differs from the translational one [6, 7]. This case corresponds to the nonequilibrium dissociation of diatomic molecules. At $T<7000$ K the majority of modern models give similar results for the function $\varphi_q(T, T_j)$ [7].

However, there are processes proceeding behind the shock front in which two vibrationally excited molecules participate and the reaction products may form in vibrationally excited states (for example, $A_2(V)+BC(V')=AB(W)+AC(W')$). In this case both forward and backward reaction rate constants depend on at least two vibrational temperatures and the number of vibrational temperatures is greater ($j=1... n$) than two if triatomic H_2O, NO_2, and N_2O molecules participate in the reaction.

A model making it possible to take into account the effect of several vibrational temperatures differing from the translational temperature was developed for dissociation reactions in [8]. This model can fairly readily be generalized to the case of exchange reactions. In this model

$$\varphi_q(T, T_j) = \prod_{j=1}^{b_q}(1 - y_{j0})^{-g_j} \left(\prod_{j=1}^{b_q}(1 - y_j)^{-g_j} \right)^{-1} \times \exp\left[\frac{E_q^*}{k} \left(\frac{1}{T} - \sum_{j=1}^{b_q} \beta_{qj}^2 \left(\sum_{j=1}^{b_q} \beta_{qj}^2 T_j \right)^{-1} \right) \right].$$

Here, k is the Boltzmann constant and E_q^* is the energy corresponding to the vibrational level which forms a "bottleneck" in the transition of the excited molecules into a quasi-continuous (with respect to energy) continuum as a result of the chemical reaction. The quantity E_q^* depends mainly on the chemical reaction activation energy. Within the framework of the truncated harmonic oscillator model E_q^* corresponds to the energy of the last discrete level from which the dissociation proceeds. In the present paper its value was determined as in [9].

Results and discussion

Let us consider the effect of the excitation of molecular vibrations behind a shock front on the gasdynamic parameters and the concentrations of the components in the relaxation zone of a strong shock wave propagating in air which does not contain any particles at an altitude $H_0=30$ km for $M_0=10$ and $\beta=60°$. In the case when $\tau_V \leq \tau_{ch} \sim \tau_e \sim \tau_R \sim \tau_i < \tau_{ph}$, the electronically excited species and ions rapidly form behind the shock front.

Fig. 1 shows graphs of the functions $T(x)$, $p(x)$, and $M(x)$ predicted by taking into account the mutual effect of the chemical reaction kinetics and the vibrational energy exchange (thermally nonequilibrium model) and by taking into account only the chemical reactions (thermally equilibrium model). Clearly, taking into account the delayed excitation of the vibrations and its effect on the chemical reaction rates significantly affects the dynamics of variation of T, p, and M in the relaxation zone.

For the thermally nonequilibrium model the main features of the behaviour of $T(x)$, $p(x)$, $M(x)$ are an increase in the characteristic lengths of all the processes and a considerable increase in the relaxation zone length, l_r, sharper variation of T, p, M in the relaxation zone, and significantly smaller equilibrium values of T and p and, conversely, a greater value of M at the end of the relaxation zone.
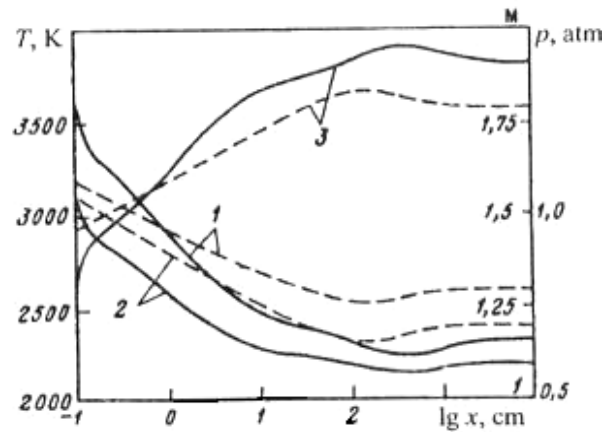
Figure. 1. Variation of T, p, and M (curves 1-3, respectively) in the relaxation zone of a shock wave calculated on the basis of the complete thermally nonequilibrium model (solid curves) and with allowance for chemical reactions only (dashed curves)

We can distinguish four characteristic regions of variation of the gasdynamic parameters in place of two regions when only the chemical reactions are taken into account. Region I is characterized by the maximum gradients of T, p, and M and begins immediately behind the shock front. In region II (more extended) the parameters T, p, and M vary more weakly (under the conditions considered the length of the region $\sim$ 10 cm). For region III still smaller gradients of T, p, and M are characteristic and its length is $\sim 3 \cdot 10^2$ cm. The extremum point of the functions $T(x)$, $p(x)$, and M(x) can be considered as a conventional right-hand limit of the third region. In region IV, which is the most extended ($\sim 2 \cdot 10^3$ cm), the sign of the derivatives dT/dx, dp/dx, and dM$/dx$ changes and at the endpoint of this region the quantities T, p, and M tend to equilibrium values. Such behaviour of the functions $T(x)$, $p(x)$, and M(x) is attributable to the characteristics of the vibrational relaxation and its effect on the chemical reaction rates.

It is worth to note that to predict the gasdynamic parameter and species concentration evolution in the shock layer in front of the vehicle moving with the supersonic velocity in the atmosphere the rather simplified thermally nonequilibrium model involving the following chemical reactions is widely applied

1. $N_2 + M = N + N + M$
2. $O_2 + M = O + O + M$
3. $N_2 + O = NO + N$
4. $O_2 + N = NO + O$
5. $NO + M = N + O + M$

Nitric oxide in this model forms due to well known Zeldovich mechanism (reactions nos 3 and 4). However, it is believed that there exist the other mechanisms of NO formation in combustion of fuel/air mixtures. One of them is connected with reactions involving NO_2 [9]

$O_2 + NO = O + NO_2$
$NO_2 + M = NO + O + M$
$NO_2 + N = 2NO$
$2NO_2 = 2NO + O_2$
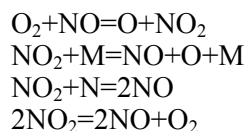
Besides N- and O-containing species the ambient atmosphere contains in a marked amount H_2O and other H-containing species [10]. Therefore, it is fruitful to take into account in the kinetic mechanism additionally the reactions involving H_2, H, H_2O, OH species. Computations exhibited that neglecting of NO_2 mechanism in NO formation process results in a significant overestimation of relaxation zone length and the final equilibrium value of NO concentration. It is clearly seen from the plots presented in Fig.2. For the kinetic mechanism involving 9 species: N, O, N_2, O_2, NO, H_2O, H_2, H, OH at $M_0 = 10$,

4

β=60°, H=30 km predicted relaxation zone length is as large as 526 m and for the reaction mechanism involving additionally processes with NO_2 (10 species) the predicted relaxation zone length is considerably smaller, l_r=38 m. The NO mole fraction at $x=l_r$ (equilibrium value of γ_{NO} further labeled as γ^e_{NO}) in this case is markedly larger, $\gamma^e_{NO}=1.47\cdot10^{-2}$, as compared to the γ^e_{NO} computed by the model taking into account the single Zeldovich mechanism of NO formation ($\gamma^e_{NO}=4.69\cdot10^{-3}$). This result exhibits that NO formation in the post shock region at moderate temperatures behind the front (T_1=3000-5000 K) is not caused by Zeldovich mechanism only.

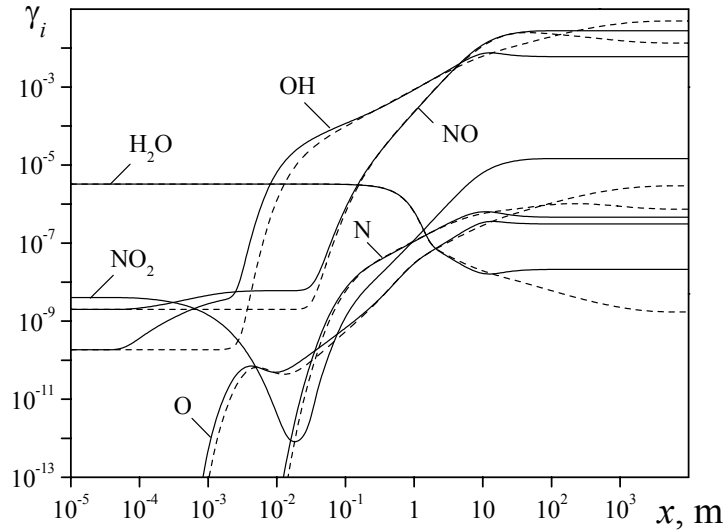Figure. 2. Variation of species mole fractions, γ_i, in the relaxation zone of a shock wave computed on the basis of thermally nonequilibrium model involving 10 species (solid curves) and model involving 9 species (dotted curves): M_0=10, β=60°, H=30 km (T_0=230 K, p_0=1.184 kPa)

Fig.3 shows the dependence of the vibrational temperatures, T_j, for O_2, N_2, NO, and NO_2, and the translational temperature T in the shock wave relaxation zone (M_0=10, β=60°, and H=30 km). Clearly, the sharp decrease in T directly behind the shock front is due to the fast excitation of the molecular vibrations of O_2. In this region the pressure also decreases and the velocity increases since in supersonic flow heat transfer from the translational degrees of freedom (the energy of the translational degrees of freedom goes over into the vibraIional ones) results in flow acceleration.

The vibrations of the N_2 molecules are excited significantly slower. It is precisely this process that mainly affects the variation of T, p, and M in the second region, although here the dissociation of O_2, which also contributes to the variation in the gasdynamic parameters, has already started. We should note that for $x < 1$ cm the temperature determined from the complete thermally nonequilibrium model is lower than the corresponding values of T calculated with thermally equilibrium one. Therefore, where as for $x < 1$ cm the slowing down of the chemical reactions as compared with the model in which the effect of vibrational relaxation is not taken into account is related to the decrease in the quantity $k_{\pm q}$ as a result of the fact that $T_j < T$, for $x > 1$ cm the decrease in $k_{\pm q}$ is due to the stronger fall in temperature.

When $x\sim10$ cm thermodynamic equilibrium is established between the vibrational and translational degrees of freedom and in the third region the variation of the gasdynamic parameters is caused only by chemical reactions proceeding with the absorption of energy (mainly the dissociation of O_2 and N_2 and the formation of NO and NO_2). When $x > 3\cdot10^2$ cm, T and p begin to increase and M to decrease. In the fourth region the variation of T, p, and M is mainly due to hydrogen atom recombination. It is worth to note that even with allowance for the slower excitation of O_2, N_2, and NO the neglect of the reactions with the NO_2 participation does not make it possible to describe the

changes in both the gasdynamic parameters and the NO concentration correctly. The distributions of T and T_j for this case are shown by the dashed curves in Fig. 3.
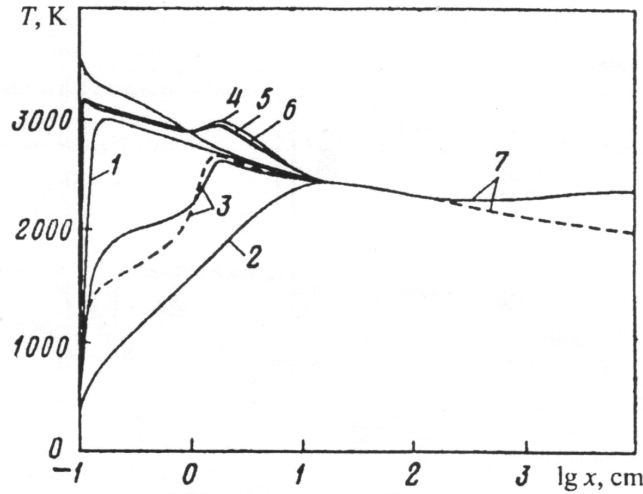

Figure 3. Variation of the vibralional temperatures of O_2, N_2, and NO (curves *1-3*), the symmetric, deformation, and asymmetric modes of NO_2 (curves *4-6*), and the translational temperature T (curve *7*) in the relaxation zone of a shock wave calculated on the basis of the complete model involving 10 species (solid curves) and the model in which reactions with NO_2 are excluded (dashed curves)

The computations show that besides usually accounting N_2, O_2, O, N, NO species [4, 5] the different excited molecules, mainly $O_2(a^1\Delta_g)$, $O_2(b^1\Sigma_g^+)$, and atoms $O^1(D)$ form in the noticeable amount behind the oblique shock front. For example, the concentration of $O_2(a^1\Delta_g)$ for the air shock wave with M_0=15, β=45°, T_0=253 K, p_0=24.12 Pa (these T_0 and p_0 values correspond to the parameters in the atmosphere at the altitude H=60 km) at 1 m distance from the front is compared with the concentration of NO. Among the charged species besides NO^+ ions and electrons the different positive (O_2^+, O^+, N_2^+, N_2O^+) and negative (O^-, O_2^-, NO_2^-, O_3^-) ions form in the relaxation zone behind the shock front. This is illustrated in Fig.4 which depicts the evolution of neutral and charged species mole fractions along the flow behind the air shock front (H=60 km). It is worth noting the model taking into account the exited species formation predicts the larger concentration of ions at the initial and the final stages of ionization process as compared to the model involving electronically unexcited species only. For instance, the difference in the concentration of NO^+ ions at the 10 cm distance from the shock attains a factor of 2. However, the maximal concentrations of NO^+ ions and electrons are close for both models.

The more intensive formation of ions in the case of taking into account the processes with electronically excited atoms and molecules is caused by lowering of a barrier of ionization reactions. The main reactions with excited atoms and molecules leading to acceleration of ion formation are: $O_2+O^+=O_2^++O(^1D)$, $N(^4S)+O(^1D)=NO^++e$, $N(^4S)+O(^1S)=NO^++e$, $O^-+O_2(b^1\Sigma_g^+)=O+O_2+e$, $O^-+O_2(a^1\Delta_g)=O_3+e$, $O_2^-+O_2(a^1\Delta_g,b^1\Sigma_g^+)=2O_2(X^3\Sigma_g^-)+e$. These reactions occur much faster than the corresponding ones with unexcited atoms and molecules.

Consider now the case when nanoparticles present in the ambient air. Meteoric dust, multi-ion complexes, radical clusters, and Aitken nuclei are the main particles with the size of several nanometres that are observed in the upper and middle atmosphere [11]. The concentration of these particles is around 10^3-10^4 cm^{-3}. The size particle distribution is supposed to be lognormal with median radius $\bar{a}$=10 nm and geometric deviation σ=1.25. The primary particles are supposed to be neutral and total particle concentration is taken N_0=10^4 cm^{-3}. Formation of a large amount of electrons and ions in the shock layer (for M_0=15, β=45°, H=60 km the maximal concentration of electrons and NO^+ ions attains at 1 m distance from shock front and is as large as N_i=3·10^8 cm^{-3}) leads to fast charging of

particles. The coefficient of attachment of the ion to the particle, $\beta_i^{(P)}$, depends on the P parameter, polarities of particle and ion, radius of the particle, temperature, and ion mass.
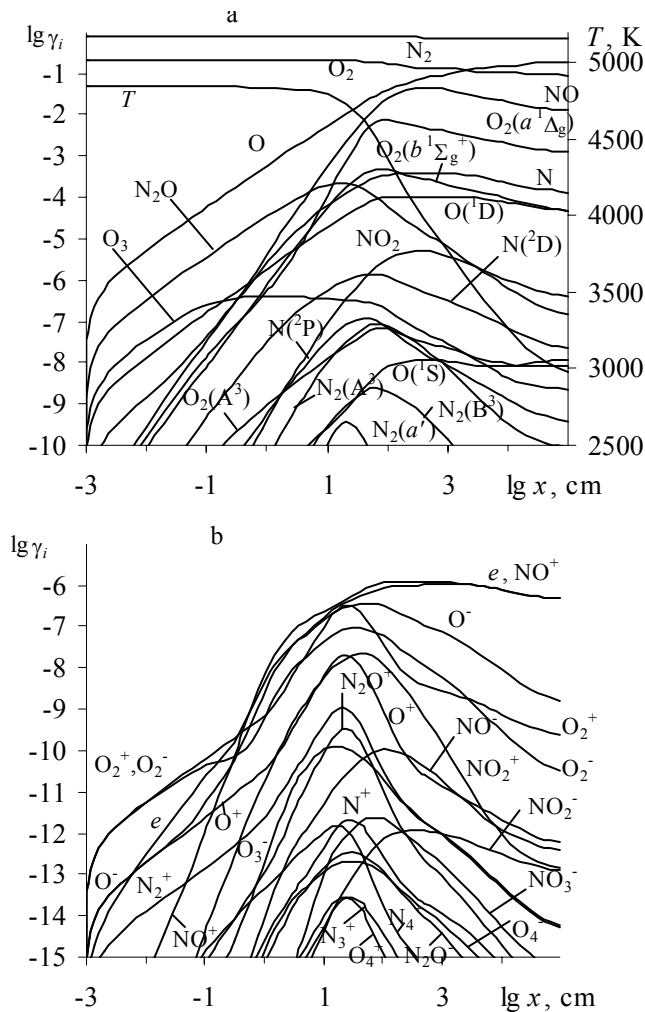

Figure 4. Evolution of temperature and mole fractions of neutral species (including electronically excited ones) (a) and different ions (b) behind the shock front at T_0=253 K, p_0=24.12 Pa, M_0=15, β=45°

Due to the smaller mass of electron as compared to mass of any ion the attachment coefficient for electron is much higher than one for ions. The $\beta^{(P)}$ value for NO^+ ion and particle with a=10 nm, at P=0, T=3500 K is as large as 10^{-6} cm^{-3}/s, and time of charging, τ_c, is ~10^{-2} s for ion and τ_c~10^{-5} s for electron. The rapid attachment of electrons to particles results in the formation of an ensemble of negatively charged particles. The dynamics of particle charging behind oblique air shock front for M_0=15, β=45°, H=60 km is illustrated in Fig.5. It is clearly seen that behind the shock front the primary neutral particles acquire a significant charge: at 1 m distance from the front the concentration of particles, $N(q)$, with charge q=-12 is around 10^3 cm^{-3}. The particles with larger and smaller negative charge arise. The larger particles with a=20 nm may acquire q=14e and small size particles with a≤6 nm may accumulate only 8-10 elementary charges. Fig.6 shows the predicted charge distribution of particles with different radius for flow parameters considered above.
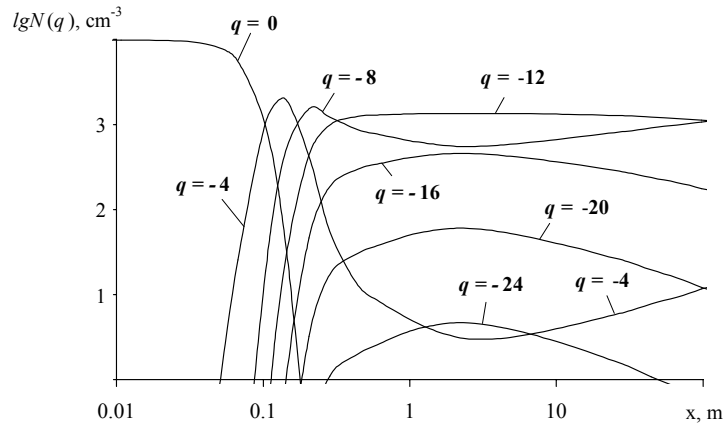
Figure 5. Evolution of charged particle concentration with given charge, q, along the flow behind shock front at $M_0=15$, $\beta=45°$, $T_0=253$ K, $p_0=24.12$ Pa, $N_0=10^4$ cm^{-3}

Because in the case considered $N_i \gg N_0$ the presence of particles in the air shock wave plasma does not lead to a noticeable change in the ion (electron) concentration. However, in the case when $N_i \approx N_0$, the charging of particles results in a significant reduction in ion concentration. The condition $N_i \approx N_0$ may be met upon formation of nanoparticles and clusters in a shock layer due to ablation or erosion of vehicle thermal protection. The variation of plasma properties in this case should be taken into account.
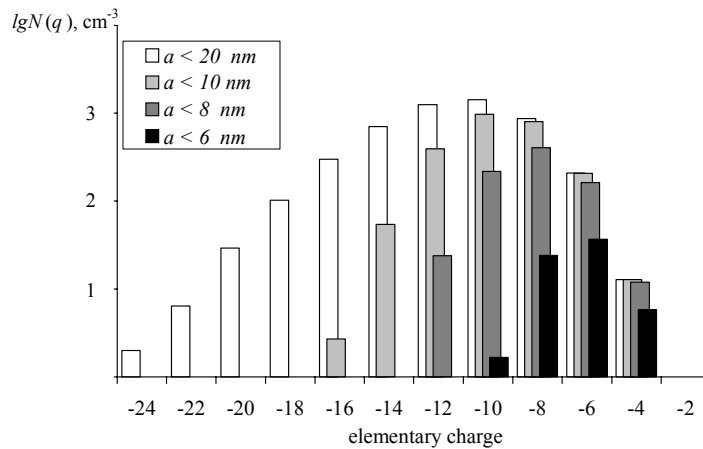

Figure 6. Charge distribution of nanoparticles with radius smaller than given value at 50 cm distance behind shock front for $M_0=15$, $\beta=45°$, $T_0=253$ K, $p_0=24.12$ Pa, $N_0=10^4$ cm^{-3}

Fig.7 shows the variation of concentration of positive and negative ions and electrons behind the front of shock wave for the case when $N_i \geq N_0$. At H=60 km, $M_0=13$, and $\beta=45°$ this condition is satisfied for $N_0=10^8$ cm^{-3}. For flow parameters behind the front: $T_1=3750$ K, $p_1=2.5$ kPa the maximal concentrations of positive ions and electrons at $N_0=0$ (no particles in the flow) are $N_i^+=N_e=4\cdot10^9$ cm^{-3}. In the case of abundance of nanoparticles in the shock layer ($N_0=10^8$ cm^{-3}) the maximal concentrations of negative and positive ions and electrons are considerably smaller: $N_i^-=4.7\cdot10^7$ cm^{-3}, $N_i^+=1.5\cdot10^9$ cm^{-3}, $N_e=1.7\cdot10^8$ cm^{-3}. The difference in the concentrations is caused by charging of particles.

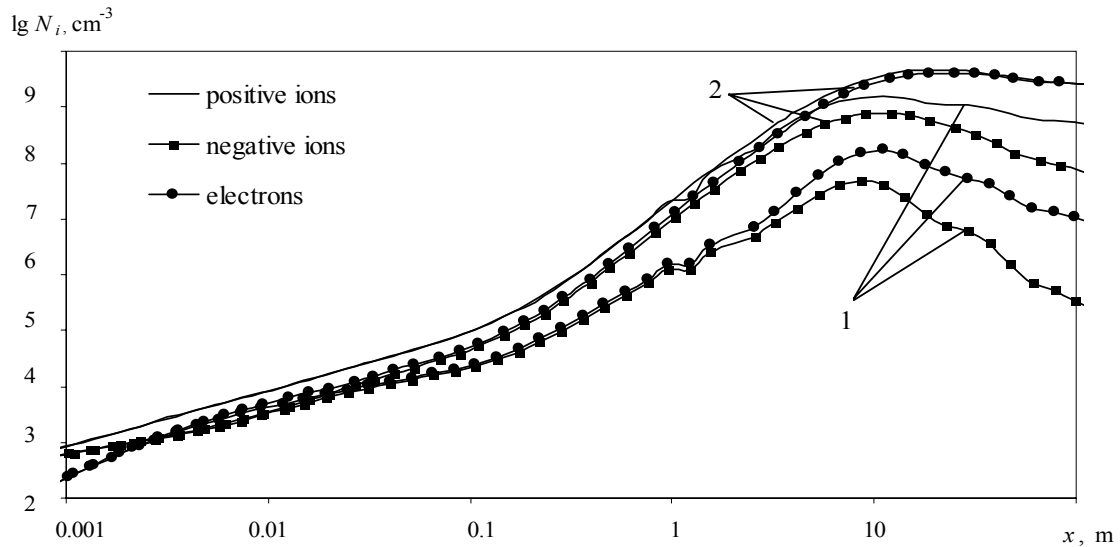Figure 7. Evolution of positive and negative ion and electron concentrations in the relaxation zone of a shock wave at M_0=13, β=45°, H=60 km in the cases of abundance of nanoparticles in the shock layer (curves 1) and upon absence of nanoparticles (curves 2)

Charged particles with opposite polarities coagulate much faster than neutral ones [12]. For example, the enhancement factor for the coagulation rate caused by Coulomb interaction for particle with a_1=1 nm, q_1=+2e and particle with a_2=10 nm, q_2=-15e is as large as 15.2. The coagulation rate for these particles at temperature T=3500 K and pressure p=10^3 Pa attains 0.64·10^{-7} cm^3/s. At total particle concentration behind the shock N_0=10^6 cm^{-3} the coagulation time is around 1.5 s. Therefore, the coagulation may change the size particle distribution at the stagnation point region only where the plasma residence time is much larger. It is worth to note that polarization interaction of small size particle with large size particle having the same polarities can enhance the coagulation, additionally. The coagulation between particles with the same polarities or between charged and neutral particles may also occur due to difference in the intensity of ion flux to particles with different sizes and charges and due to exerting of striction force in the inhomogeneous electric field created by charged particle.

Concluding remarks

Despite the longstanding experience in the modelling and experimental studies of nonequilibrium processes behind the air shock wave some problems are from being resolved. These problems are connected mostly with the presence of clusters and nanoparticles in plasma forming in the post shock region. Computations exhibit that in practically interested range of temperature behind the front (T_1=2500-4000 K) to predict properly the relaxation zone length and evolution of charged and neutral species concentrations in the post shock region it is needed to take into account besides the well known Zeldovich mechanism also the NO_2 mechanism of NO formation and enhance of ionization processes due to abundance of the electronically excited species in the relaxation zone. Nanoparticles that present in the ambient atmosphere or form due to ablation or erosion of vehicle surface protection may acquire a significant negative charge in a shock due to attachment of ions (electrons) to particles and affect their concentrations. It allows to control the particle moving in the shock layer by external electric field and to change the properties of dusty plasma behind the shock. The further studies of these processes are strongly needed.

Acknowledgements

References

[1] Capitelli M, editor (1996) Molecular Physics and Hypersonic Flows. NATO-ASI Series C: Mathematical and Physical Sciences. V.482. Dordricht. NL: Kluwer Academic Publishers

[2] Sarma GSR (2000) Physico-Chemical Modeling in Hypersonic Flow Simulation. Progress in Aerospace Sciences, Vol.36, pp.281-349

[3] Savel'ev AM, Starik AM, Titova NS, and Favorskii ON (2004) Mechanism of the Electric Charging of Soot Particles upon the Combustion of Hydrocarbon Fuels. Doclady Physics, Vol.49, No.8, pp.441-446

[4] Knab O, Frühauf H-H, and Messerschmid EW (1995) Theory and Validation of Physically Consistent Coupled Vibration-Chemistry Vibration Model. Journal Thermophysics and Heat Transfer, Vol.9, No.2, pp.219-226

[5] Olejniczak J and Candier GV (1995) Vibrational Energy Conservation with Vibrational-Dissociation Coupling: General Theory and Numerical Studies. Physics Fluid, Vol.7, pp.1764-1774

[6] Kovach EA, Losev SA, and Sergievskaya AL (1995) Two-Temperature Chemical Kinetics Models for Describing Molecular Dissociation in Strong Shock Waves. Chim. Fiz, Vol.14, No.9, p.44

[7] Losev SA, Sergievskaya AL, Rusanov VD et al. (1996) Nonequilibrium Factor in Two-Temperature Dissociation Kinetics Behind a Shock Front. Dokl. Ros. Akad. Nauk, Vol.346, p.192

[8] Kuznetsov NM (1982) Kinetics of Monomolecular Reactions [in Russian], Nauka, Moscow

[9] Dautov NG, Starik AM (1997) On the Problem of Choosing a Kinetic Scheme for the Homogeneous Reaction of Methane with Air. Kinetics and Catalysis, Vol.38, No.2, pp.185-208

[10] Shimazaki T (1984) The Photochemical Time Constants of Minor Constituents and Their Families in the Middle Atmosphere. Journal Atmospheric and Terrestrial Physics. Vol.46, No.2, pp.173−191

[11] Prather MJ, Wesoky HL, Miake-Lye RC et al. (1992) The Atmospheric Effect of Stratospheric Aircraft: A First Program Report. NASA Reference Publications 1272

[12] Seinfeld JH and Pandis SP (1998) Atmospheric Chemistry and Physics, Willey, New York